



# A Clinical Measuring Platform for Building the Bridge Across the Quantification of Pathological N-Cells in Medical Imaging for Studies of Disease

Peifang Guo<sup>(✉)</sup>

Montreal, QC, Canada  
peif.guo@gmail.com

**Abstract.** In this paper, a clinical measuring platform for quantifying nucleus-cells (MPQ-N-cells) at combining a novel color region-based segmentation strategy is proposed to accelerate the discovery of diseases diagnostically in medical imaging. In the approach, average values of colors in an image are employed as similarity criteria to assign image voxels to regions using the minimum distance classifier in the color region growing process. Then, the binary image transformation and graphic contour line procedure are performed, followed by the operation of region area calculation to obtain the actual numbers of voxels within the segmented patterns of the N-cells quantitatively. The proposed approach of MPQ-N-cells is implemented on the heterogeneous medical image datasets related to Parkinson disease, oculopharyngeal muscular dystrophy (one type of protein conformational diseases) and glioblastoma cancer. Implementation results reveal that the proposed MPQ-N-cells approach is capable of quantifying a variety of pathological N-cells clinically with improved data visualization in heterogeneous datasets. This study has the potential to lead to more successful measurement of cell diagnostically and further to track changes of cell in medical imaging for a longitudinal study on supporting the studies of disease.

**Keywords:** Pathological nucleus cells measurement · Color region-based segmentation · Region area calculation · Binary image transformation · Graphic contour line procedure · Minimum distance classifier · Parkinson disease-related protein · Glioblastoma · Protein conformational diseases

## 1 Introduction

Numerous human diseases, such as Parkinson disease (PD) and protein conformational diseases (PCDs), have characteristic pathologic signatures involving the accumulation of particular protein as extracellular deposits or intracellular inclusions in certain organs. In general, the deposits of abnormal protein accumulation have the appearance of nucleus-cells (N-cells) in medical imaging (Fereshtehnejad et al. 2017; Tanti et al. 2014; Hortin et al. 2010; Blumen et al. 2009). Medical studies also show that brains of people with glioblastoma cancer, one of the most aggressive malignant primary tumors

among 120 different types of brain tumors, are composed of spongioblasts with the shape of N-cells pathologically in medical imaging (Raghavendra et al. 2018; Gerard et al. 2017; Egger, et al. 2013; Bauer, et al. 2013).

Medical images in different modality are able to exhibit different characteristic information of human body and pathological changed tissue of N-cells related to diseases. In general, associated with other clinical factors and disease symptoms, the stages of disease could be defined approximately by the degree of N-cells spread in medical imaging. Usually, the higher amounts of pathological N-cells are correlated with aggressive diseases, compared to the early stage cases. Hence, an approach to quantifying pathological N-cells at combing the visualization of segmented N-cells spread in imaging could serve as a stage indicator for a reference in differentiating between early stage and advanced (aggressive) diseases related to PD, PCDs and glioblastoma cancer for disease diagnosis (Guo 2017; Gerard et al., 2017; Blumen et al. 2009).

Due to the presence of image noise in the mage acquisition process, similar characteristics of normal and some abnormal tissue of N-cells may cause interpretational errors in medical imaging. In addition, the huge amount of medical image data produced by imaging devices makes the measurement of potential diseases of N-cells a heavy task in clinical settings (Bakas, et al. 2017; Duyn 2012; Hortin, et al. 2010). It is useful to design a platform for the segmentation of abnormalities of N-cells followed by the measurement of segmented patterns of N-cells subsequently in medical imaging (Guo et al. 2018; Ahmed et al. 2015; Gui et al. 2012). This study seeks to address the issue of measuring pathological N-cells quantitatively at combining a novel color region-based segmentation strategy in the heterogeneous medical imaging, related to PD, one type of PCDs, oculopharyngeal muscular dystrophy (PCDs-OPMD) and glioblastoma cancer on supporting the studies of disease.

## 2 Proposed Platform

There are different methodologies for image segmentation of N-cells in the literature, including the deep learning based algorithms using image markers (Al-Kofahi et al. 2018; Pärnamaa et al. 2017), the graphical model methods (Murphy 2010; Deshmukh et al. 2014), the threshold-based techniques (Wang et al. 2014; Rafael et al. 2008; Ostu 1979), the level set method (Dzyubachyk et al. 2008). Most of methodologies above rely on the information of shapes of N-cells, which would be applicable only when the appropriate shapes of N-cells in images are available (Rafael et al. 2008; Tohka 2014). Unlike the methodologies of segmentation reviewed above, this study designs the color region-based segmentation strategy to extract disease-related-patterns of N-cells for quantifying segmented patterns of N-cells with irregular shape in medical imaging.

The goal of color region-based segmentation is to divide an image into a set of non-overlapping regions of similar attributes with color. Figure 1 shows a clinical measuring platform for quantifying N-cells (MPQ-N-cells) via a novel strategy of color region-based segmentation with data visualization in medical imaging on supporting the diagnoses of disease. In a color image, each voxel will be represented as a vector of the red, green and blue components (RGB-c) from the origin to that voxel point in the space of RGB-c. Starting from computing the average of colors in the RGB-c for

regions of pattern in an image, the proposed MPQ-N-cells then employs the average values of color in the RGB-c as the similarity criterion to assign voxels in regions in the region growing process. When the similarity criterion is satisfied with the minimum distance classifier, the voxel will be assigned in that region, indicating that the voxel most closely matches that color of the region in the space of RGB-c in segmentation.

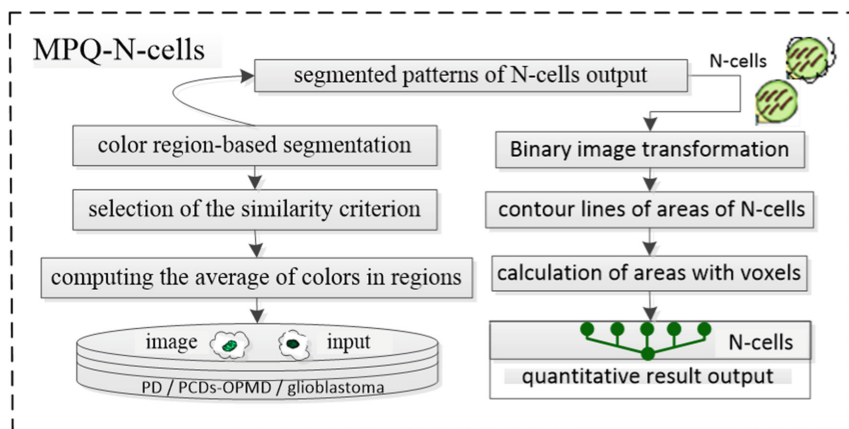


**Fig. 1.** Proposed platform.

Further, together with the steps of binary image transformation and graphic contour line procedure, the operation of region area calculation is accomplished to obtain the actual numbers of voxels within the segmented patterns of the N-cells quantitatively. In the validation stage, the MPQ-N-cells approach is implemented on heterogeneous medical image datasets, including the PD-related protein image, the microscopy images of PCDs-OPMD and the multi-photon microscopy images of glioblastoma cancer.

### 3 Implementation Results

The PTEN-induced putative kinase 1 (PINK1) is a serine protein kinase which is implicated in protecting cells from stress-induced mitochondrial dysfunction. Mutations in this gene are thought to be the cause of autosomal recessive early-onset Parkinson disease 6 (PARK6) (Tanti et al. 2014; Hortin et al. 2010). Figure 2 presents the segmentation results from an example of experiments in the MPQ-N-cells implementation in the medical image, where the PD-related protein PINK1 was in the process of presenting mitochondrial antigens with red color for the immune system. Figure 2(a) is the original PD-related protein image (Image credit: The Neuro) with two different colors, red and green. Achieved from the MPQ-N-cells implementation in this study, Fig. 2(b)–(c) are the segmentation results with the output of two extracted image

patterns of N-cells, the segmented cell of mitochondrial antigens with red in Fig. 2(b) and the segmented cell of intact mitochondria with green in Fig. 2(c) (both segmented image patterns in Fig. 2(b)–(c) need to be measured quantitatively further in this study).

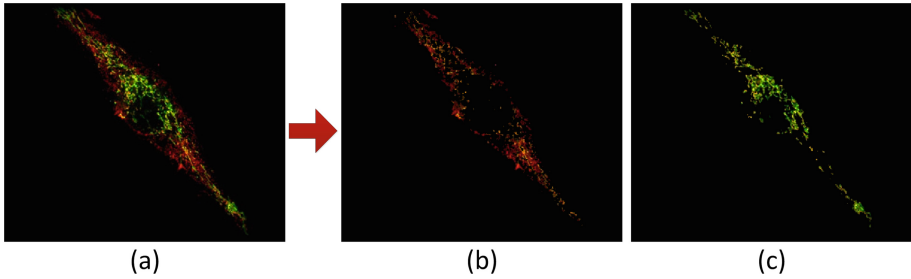


**Fig. 2.** Segmentation results from an example of experiments from the MPQ-N-cells implementation in the PD-related protein image: (a) original PD-related protein image; (b) segmented mitochondrial antigens with red (c) segmented intact mitochondria with green. (Color figure online) *The Neuro*

Each proteopathy of PCDs is characterized by a disease-specific buildup of aggregated proteins within tissue of the body. For the type of PCDs, oculopharyngeal muscular dystrophy (PCDs-OPMD), the Poly(A)-Binding Protein 1 (PABPN1) induces the formation of N-cells of muscular intranuclear inclusions (MII) that are the pathological biomarkers of PCDs-OPMD (Blumen et al. 2009; Hortin et al. 2010). Figure 3 shows two examples of the experiments in the MPQ-N-cells implementation on the microscopic image data of PCDs-OPMD. Figure 3(a) is the two original microscopic images of PCDs-OPMD (Image credit: the Centre Hospitalier de l'Université de Montréal), where the N-cells of MII show the light green color. Achieved from the MPQ-N-cells implementation, the segmentation results are shown in Fig. 3(b)–(e) with the output of the four extracted image patterns, the image background with black color in Fig. 3(e), the two layers with various dark green colors in Fig. 3(c)–(d) and the MII cells with light green color in Fig. 3(b) (needs to be measured quantitatively further in this study).

Glioblastoma is a fast-growing malignant brain tumor composed of spongioblasts (Menze et al. 2015; Egger, et al., 2013). Figure 4 shows the segmentation results from two examples of experiments in the MPQ-N-cells implementation in multi-photon microscopy images of glioblastoma. Figure 4(a) is the two original images of glioblastoma (Image credit: Raghavendra et al. 2018) with two different colors of patterns, the glioblastoma cells in green and image markers in white. Achieved from the MPQ-N-cells implementation, the segmentation results are shown in Fig. 4(b)–(c) with the output of the two segmented image patterns, the segmented patterns of markers with white in Fig. 4(c) and the segmented patterns of glioblastoma cells with green in Fig. 4(b) (needs to be measured quantitatively further in this study).

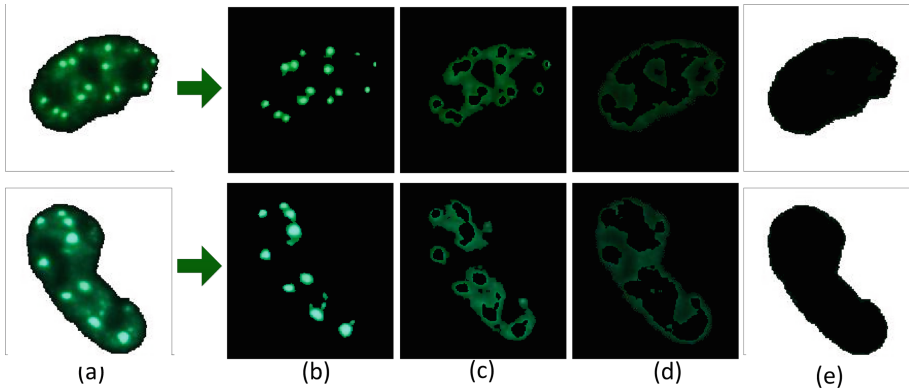


**Fig. 3.** Segmentation results from two examples of experiments from the MPQ-N-cells implementation on the PCDs-OPMD data: (a) two original microscopic images of PCDs-OPMD; (b) segmented MII cells with light green; (c)–(d) two segmented layers with various dark greens; (e) the background with black. (Color figure online) the Centre Hospitalier de l'Université de Montréal

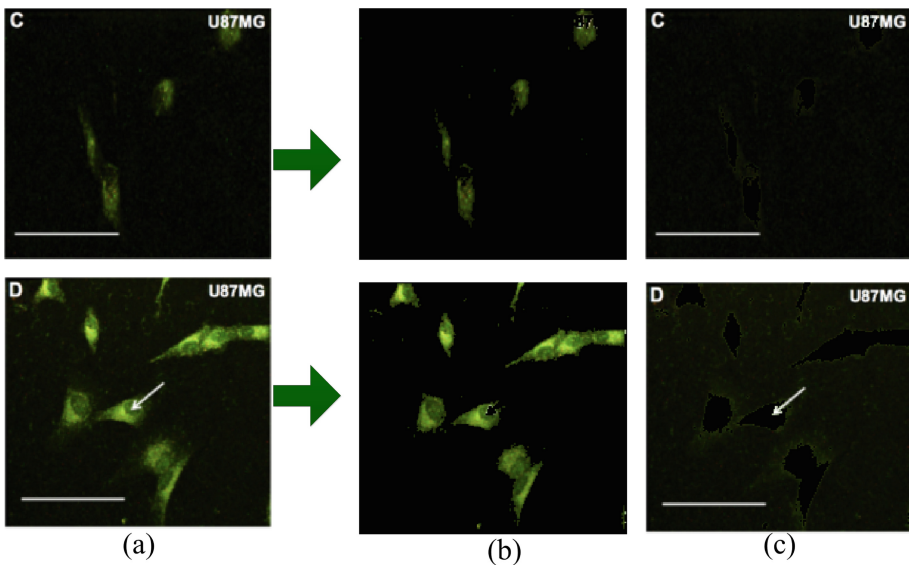


**Fig. 4.** Segmentation results from two examples of experiments in multi-photon microscopy images of glioblastoma; (a) two original images of glioblastoma; (b)–(c) segmented glioblastoma cells in green and segmented image markers in white, both achieved from the MPQ-N-cells implementation in this study. (Color figure online) Raghavendra et al. 2018

Achieved from the MPQ-N-cells implementation, Figs. 5, 6 and 7 show further the results of the binary image transformation with the output of graphic contour lines for quantifying the six resulting segmented-patterns of various N-cells, i.e., the two

segmented cells of mitochondrial antigens and intact mitochondria from Fig. 2(b)–(c), the two segmented MII cells from the column of Fig. 3(b) and the two segmented glioblastoma cells from the column of Fig. 4(b). Figures 5, 6 and 7(b) display their binary image representations in a logical array of 0 s and 1 s for computing the actual numbers of voxels within the segmented N-cells, while Figs. 5, 6 and 7(c) illustrate the output of graphic contour lines which sketch the bounding areas of the segmented N-cells with voxels for the measurement purpose.

Using the operation of region area calculation, Table 1 reports the quantitative results for the actual numbers of voxels within the six segmented-patterns of N-cells in Figs. 5, 6 and 7(a) {i.e., the bounding areas of the red/green regions within the two PD-related protein cells in Fig. 5(a), the bounding areas of the light green region within the two MII cells in Fig. 6(a) and the bounding areas of the green region within the two glioblastoma cells in Fig. 7(a)}. From Table 1, it can be observed that the image subject with N-cells of glioblastoma in the 2nd row of Fig. 7 is more progressive and aggressive with the number of 2846, spreading more extensively by 207.34% as compared to the other image subject with N-cells of glioblastoma in the 1st row of Fig. 7 with the number of 926  $\{(2846-926)/926 = 2.0734\}$ ; this would be useful for assessing the stages of disease quantitatively for patients with glioblastoma cancer in the disease diagnosis.

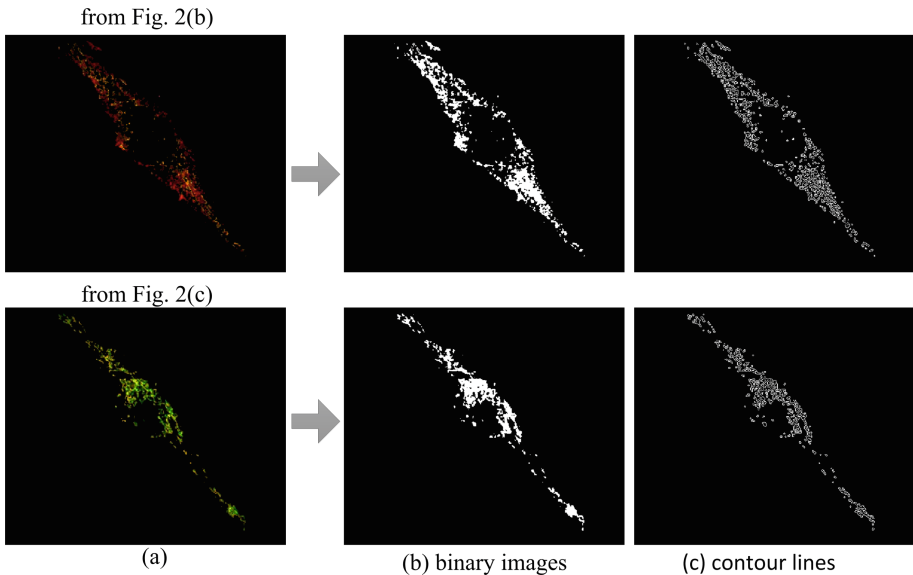


**Fig. 5.** Results of the binary images of the segmented PD-related protein cells with the output of graphic contour lines from the PD-related protein image in the MPQ-N-cells implementation.

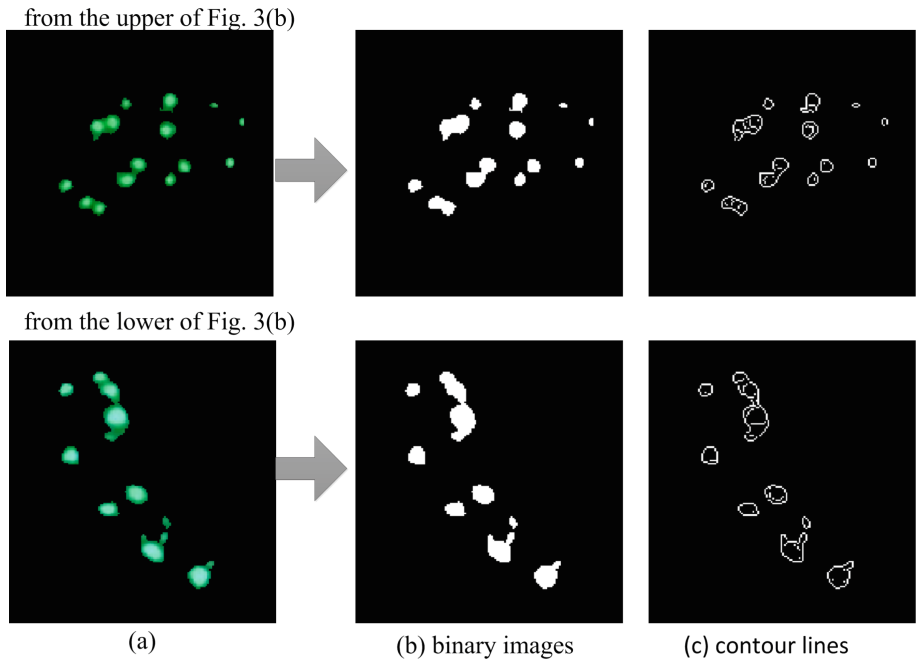


**Fig. 6.** Results of the binary images of segmented MII cells with their contour line output from two examples of experiments on the PCDs-OPMD data in the MPQ-N-cells implementation.

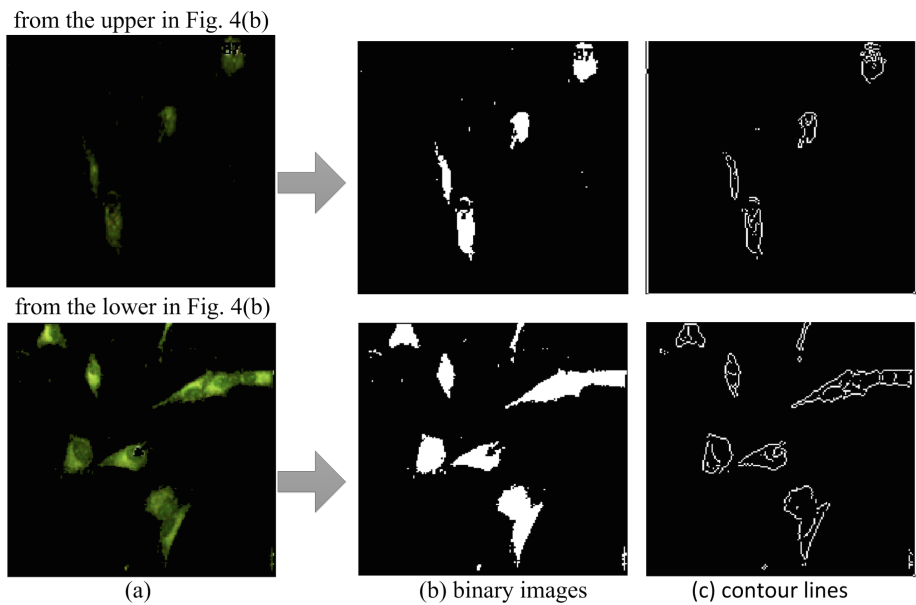


**Fig. 7.** Results of the binary images of segmented glioblastoma cells with their contour line output from two examples of experiments in multi-photon microscopy images of glioblastoma in the MPQ-N-cells implementation.

**Table 1.** Quantitative results for measuring the six segmented patterns of N-cells related to diseases in Figs. 5, 6 and 7.

Measuring N-cells	PD-related protein	Figure 5 (a)	MII	Figure 6 (a)	glioblastoma	Figure 7 (a)
	Upper	Lower	Upper	Lower	Upper	Lower
#voxels in area of N-cells	6390	4306	860	1162	926	2846

## 4 Conclusion

In this study, without the prior knowledge of shapes of N-cells, the proposed MPQ-N-cells performs very well in the segmentation of irregular shapes of N-cells for measuring the patterns of N-cells related to PD, PCDs-OPMD and glioblastoma on the heterogeneous image datasets. The implementation results demonstrate the benefits of the design of the MPQ-N-cells, which is capable of providing simultaneously qualitative segmentation and quantitative measures of N-cells from the medical imaging. As the author is aware that experimental results in this study in measuring a variety of pathological N-cells with improved color visualization on the heterogeneous medical image datasets have not yet been reported in the literature in a comparable image cell-pattern segmentation scenario.

This study mainly focuses on the medical image data associated with the diseases of PD, PCDs-OPMD and glioblastoma cancer. Although the current proposed MPQ-N-cells has a limitation of the shortage of image data used in the implementation, this can be solved by implementing more medical images with access to big data. The future work will focus on presenting more results by conducting more experiments in big data sets, further develop the proposed approach to tracking the changes of cell for a longitudinal study on supporting the diagnoses of disease in medical imaging.

## References

- Ahmed, W., Fan, L.: Analyze physical design process using big data tool: hidden patterns, performance measures, predictive analysis and classifying logs. *Int. J. Softw. Sci. Comput. Intell.* **7**(2), 31–49 (2015)
- Al-Kofahi, Y., Zaltsman, A., Graves, R., Marshall, W., Rusu, M.: A deep learning-based algorithm for 2-D cell segmentation in microscopy images. *BMC Bioinformatics* **19**(365), 1–11 (2018)
- Bauer, S., Wiest, R., Nolte, L.-P., Reyes, M.: A survey of MRI-based medical image analysis for brain tumor studies. *Phys. Med. Biol.* **58**, R97–R129 (2013)
- Bakas, S., et al.: Segmentation labels and radiomic features for the pre-operative scans of the TCGA-GBM collection. *The Cancer Imaging Archive* (2017)
- Blumen, S.C., et al.: Cognitive impairment and reduced life span of oculopharyngeal muscular dystrophy homozygotes. *J. Neurology* **73**(8), 596–601 (2009)
- Duyn, J.H.: The future of ultra-high field MRI and fMRI for study of the human brain. *Neuroimage* **62**, 1241–1248 (2012)



- Deshmukh, B.S., Mankar, V.H.: Segmentation of microscopic images: A survey. In: International Conference Electronic Systems, Signal Processing and Computing Technologies, pp. 362–366 (2014)
- Dzyubachyk, O., Niessen, W., Meijering, E.: Advanced level-set based multiple-cell segmentation and tracking in time-lapse fluorescence microscopy images. In: IEEE International Symposium on Biomedical Imaging: From Nano to Macro, pp. 185–188 (2008)
- Egger, J., et al.: GBM volumetry using the 3D slicer medical image computing platform. *Sci. rep.* **1364**, 1–7 (2013)
- Fereshtehnejad, S.M., Zeighami, Y., Dagher, A., Postuma, R.B.: Clinical criteria for subtyping Parkinson's disease: biomarkers and longitudinal progression. *Brain* **140**(7), 1959–1976 (2017)
- Guo, P., Evans, A., Bhattacharya, P.: Nuclei segmentation for quantification of brain tumors in digital pathology images. *Int. J. Softw. Sci. Comput. Intell.* **10**, 36–49 (2018)
- Guo, P.: A tissue-based biomarker model for predicting disease patterns. *J. Knowl. Based Sys.* **276**, 160–169 (2017)
- Gui, L., Lisowski, R., Faundez, T., Huppi, P.S., Lazeyras, F., Kocher, M.: Morphology-driven automatic segmentation of MR images of the neonatal brain. *Med. Image Anal.* **16**, 1565–1579 (2012)
- Gerard, I.J., Kersten-Oertel, M., Petrecca, K., Sirhan, D., Hall, J.A., Collins, D.L.: Brain shift in neuronavigation of brain tumours: a review. *Med. Image Anal.* **35**, 403–420 (2017)
- Hortin, G.L., Carr, S.A., Anderson, N.L.: Introduction: advances in protein analysis for the clinical laboratory. *Clin. Chem.* **56**, 149–151 (2010)
- Menze, B.H., et al.: The multimodal brain tumor image segmentation benchmark (BRATS). *IEEE Trans. Med. Imaging* **34**, 1993–2024 (2015)
- Murphy, R.F.: Communicating subcellular distributions. *Cytometry, Part A* **77A**, 686–692 (2010)
- Otsu, N.: A threshold selection method from gray-level histograms. *IEEE Trans. Syst. Man Cybern.* **9**, 62–66 (1979)
- Pärnamaa, T., Parts, L.: Accurate classification of protein subcellular localization from high-throughput microscopy images using deep learning. *Gene Genomes Genet* **7**(5), 1385–1392 (2017)
- Rafael, R.C., Wood, R.E.: *Digital Image Processing*, 3rd edn. Prentice Hall, NJ (2008)
- Raghavendra, A.J., et al.: Three-photon imaging using defect-induced photoluminescence in biocompatible ZnO nanoparticles. *J. Nanomedicine* **13**, 4283–4289 (2018)
- Tohka, J.: Partial volume effect modeling for segmentation and tissue classification of brain magnetic resonance images: a review. *World J Radiol.* **11**, 855–864 (2014)
- Tanti, G.K., Goswami, S.K.: SG2NA recruits DJ-1 and Akt into the mitochondria and membrane to protect cells from oxidative damage. *Free Radical Biol. Med.* **75**, 1–13 (2014)
- Wang, J., et al.: Multi-atlas segmentation of subcortical brain structures via the AutoSeg software pipeline. *Front. Neuroinform.* **8**, 7 (2014). <https://doi.org/10.3389/fninf.2014.00007>